

# Q-HyViT: Post-Training Quantization for Hybrid Vision Transformers with Bridge Block Reconstruction

Jemin Lee<sup>1</sup>, Yongin Kwon<sup>1</sup>, Jeman Park<sup>1</sup>, Misun You<sup>1</sup>, Sihyeong Park<sup>2</sup>, Hwanjun Song<sup>3\*</sup>

<sup>1</sup>ETRI, <sup>2</sup>KETI, <sup>3</sup>Naver AI Lab

{leejaymin,yongin.kwon,jeman,msyu}@etri.re.kr , sihyeong@keti.re.kr, ghkswns91@gmail.com

## Abstract

Recently, vision transformers (ViTs) have superseded convolutional neural networks in numerous applications, including classification, detection, and segmentation. However, the high computational requirements of ViTs hinder their widespread implementation. To address this issue, researchers have proposed efficient hybrid transformer architectures that combine convolutional and transformer layers with optimized attention computation of linear complexity. Additionally, post-training quantization has been proposed as a means of mitigating computational demands. For mobile devices, achieving optimal acceleration for ViTs necessitates the strategic integration of quantization techniques and efficient hybrid transformer structures. However, no prior investigation has applied quantization to efficient hybrid transformers. In this paper, we discover that applying existing PTQ methods for ViTs to efficient hybrid transformers leads to a drastic accuracy drop, attributed to the four following challenges: (i) highly dynamic ranges, (ii) zero-point overflow, (iii) diverse normalization, and (iv) limited model parameters (<5M). To overcome these challenges, we propose a new post-training quantization method, which is the first to quantize efficient hybrid ViTs (MobileViTv1, MobileViTv2, Mobile-Former, EfficientFormerV1, EfficientFormerV2) with a significant margin (an average improvement of 8.32% for 8-bit and 26.02% for 6-bit) compared to existing PTQ methods (EasyQuant, FQ-ViT, and PTQ4ViT). We plan to release our code at <https://github.com/Q-HyViT>.

## Introduction

Thanks to self-attention that captures the global representation and shows better generalization with a low inductive bias, vision transformers (ViTs) have substituted convolutional neural networks (CNNs) in numerous applications, such as image classification, object detection, and instance segmentation (Han et al. 2022; Khan et al. 2022). Despite the great success of ViT, the high computational requirement of ViTs still remains a significant impediment to their widespread implementation.

To democratize the ViT on resource-constrained devices, researchers have proposed a *hybrid* vision transformer architectures, where convolutional and transformer layers are combined, such as MobileViTv1 (Mehta and Rastegari

2021), or optimized attention computation is used for linear complexity, such as MobileViTv2 (Mehta and Rastegari 2022). Additionally, quantization techniques that reduce the precision of real values have been used with efficient architecture design to achieve model compression. Such quantization techniques can be categorized into two types: quantization-aware training (QAT) and post-training quantization (PTQ). While QAT offers advantages in preserving accuracy compared to PTQ, its adoption has been restricted due to privacy concerns, resource-intensive and time-consuming re-training process, and the requisite expertise for hyperparameter tuning in model architecture development (Krishnamoorthi 2018; Esser et al. 2020; Choi et al. 2018; Zhang et al. 2018; Jung et al. 2019; Zhou et al. 2016; Jacob et al. 2018a; Han, Mao, and Dally 2016).

In practical setup, PTQ methods have been more commonly employed due to their high applicability (Krishnamoorthi 2018; Jiang et al. 2021; Banner, Nahshan, and Soudry 2019; Choukroun et al. 2019; Zhao et al. 2019; Lee et al. 2018; Goncharenko et al. 2019; Migacz 2017; Wu et al. 2020b). PTQ allows pre-trained models to be calibrated without the need for re-training, using only a small unlabeled dataset. PTQ for CNN models was extensively studied, and recently, research on PTQ for vision transformers has gained significant attention. PTQ for ViTs has been shown to preserve the accuracy of quantized models by overcoming diverse activation ranges following a non-linear function. However, these studies have solely focused on pure vision transformers such as ViT (Dosovitskiy et al. 2020), DeiT (Touvron et al. 2021), and Swin (Liu et al. 2021a).

For mobile devices, achieving optimal acceleration for ViTs necessitates the fusion of quantization techniques and efficient transformer structures. However, no prior exploration exists regarding the application of quantization to efficient hybrid transformers. Although the existing PTQ can be directly applied to hybrid ViTs, this is non-trivial because of the four key differences of them from the canonical ViTs: (i) *the highly dynamic activation range* complicates accuracy preservation using existing methodologies for pure vision transformers; (ii) *the existence of bridge blocks*, which serve as connectors between convolution and transformer layers, introduces a disparity between local and global representations and the issue of zero-point overflow; (iii) *the diverse types of normalization techniques* are used in hybrid

\*Corresponding author

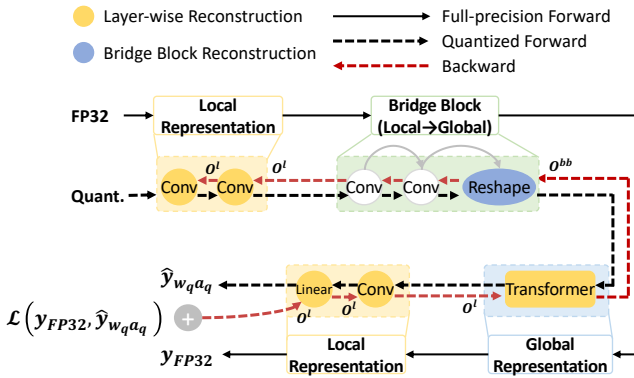


Figure 1: Overall quantization process of Q-HyViT on the representative structure of hybrid vision transformers, including local, global, and bridge representation.

vision transformers; and (iv) *the small-sized models with less than 5 million parameters* lead to a substantial loss of robustness during quantization, because of their limited number of parameters and minimal residual connections. Therefore, it is imperative to simultaneously adjust the granularity and scheme of both bridge and non-bridge layers, while also identifying the optimal scaling factors for quantization.

In this paper, we propose **Q-HyViT** in Figure 1, a tailored quantization approach for hybrid vision transformers aimed at minimizing quantization error. Q-HyViT integrates a novel *hybrid reconstruction* error minimization technique, which can determine the optimal scale factors, granularity (channel-wise or layer-wise), and quantization scheme (symmetric or asymmetric). Here, the reconstruction objective of each layer differs based on whether it is part of the bridge block<sup>1</sup> or not. To implement this technique in an integrated manner, we reuse the second-order term-based reconstruction error minimization method and extend it to incorporate the bridge block. To our knowledge, this is the *first* work that identifies the challenges of quantization for hybrid vision transformers and proposes a unified method to mitigate their errors in post-training quantization.

We conduct comprehensive experiments to compare Q-HyViT with existing open-source algorithms, namely EasyQuant (Wu et al. 2020a), FQ-ViT (Lin et al. 2022), and PTQ4ViT (Yuan et al. 2022), on the same hybrid ViT. The experiments use hybrid vision transformers including MobileViTv1 (Mehta and Rastegari 2021), MobileViTv2 (Mehta and Rastegari 2022), Mobile-Former (Chen et al. 2022), EfficientFormerV1 (Li et al. 2022), and EfficientFormerV2 (Li et al. 2023), which are representative variants of efficient vision transformers.

The results demonstrate that our Q-HyViT performs exceptionally well across five types of hybrid vision transformers and outperforms existing PTQ methods for pure ViTs (EasyQuant and PTQ4ViT) by a significant margin (up to an average improvement of 8.32% for 8-bit and 26.02% for 6-bit). Particularly, we highlight that Q-HyViT achieves state-of-the-art accuracy (an average improvement of 43.63% for

<sup>1</sup>The term “bridge block” literally refers to the transition part between convolution and transformer blocks. The precise constitution of this block slightly differs among hybrid ViT architectures.

8-bit compared with FQ-ViT) on hybrid vision transformers in *full* quantization setup, including the quantization of non-linear operations, such as softmax and normalization.

The primary contributions of our work are listed below.

- We discover that quantization of hybrid ViTs presents four unique challenges: (i) the presence of highly dynamic activation ranges, (ii) zero-point overflow in the bridge block, (iii) diverse normalization, and (iv) a parameter count of less than 5 million.
- We propose a unified method called Q-HyViT, which is based on Hessian to adjust the granularity and scheme for bridge and non-bridge layers, while also determining the optimal scaling factors for quantization.
- For comparison, we re-implement the existing PTQ methods enabling them to be applied to hybrid ViTs. We then evaluate Q-HyViT for large-scale image classification using five variants of efficient hybrid ViTs.
- Our experimental results demonstrate the effectiveness of Q-HyViT in preserving the accuracy of quantized hybrid ViTs, as it outperforms the state-of-the-art PTQ methods, FQ-ViT and PTQ4ViT.

## Related Work

Model architecture design and quantization techniques have received substantial attention in the context of efficient AI. We categorize prior research on efficient model architectures and quantization methods.

### Efficient Computer Vision Architecture

To avoid heavy computation in CNNs, standard convolutions have been replaced by separable convolutions (Chollet 2017). Separable convolutions have been widely used when designing light-weight CNNs including MobileNets (Howard et al. 2017; Sandler et al. 2018; Howard et al. 2019), ShuffleNetv2 (Ma et al. 2018), and MNAS-Net (Tan et al. 2019), reducing the computational complexity of CNN operations. Despite the prevalence of these models, a major drawback of them is that they are spatially local and have higher inductive bias than transformers.

To expand model capacity while minimizing inductive bias, a vision transformer (ViT) (Dosovitskiy et al. 2020) is employed, which directly applies a pure transformer to process image patches as a sequence. Dosovitskiy et al. (Dosovitskiy et al. 2020) showed that it performs better than CNN-based architectures on multiple image recognition benchmarks. Moreover, Touvron et al. (Touvron et al. 2021) introduced a teacher-student strategy specific to transformers, resulting in competitive convolution-free transformers trained on ImageNet only.

Even though pure vision transformer models achieve performance competitive to CNNs, the majority of these models are heavy-weight. Recently, MobileViTv1 (Mehta and Rastegari 2021), MobileViTv2 (Mehta and Rastegari 2022), EfficientFormerV1 (Li et al. 2022), EfficientFormerV2 (Li et al. 2023), and Mobile-Former (Chen et al. 2022) have been proposed for lightweight vision transformers. Such hybrid vision transformers show better accuracy than light-weight CNNs (MobileNet series) at a similar number of

model parameters by hybridizing convolution and transformers.

## Model Quantization

Quantization methods are categorized into two types: quantization-aware training (QAT) and post-training quantization (PTQ). Although QAT methods have successfully mitigated the accuracy degradation of quantized models by mapping from high-bit to low-bit precision (Krishnamoorthi 2018; Esser et al. 2020; Choi et al. 2018; Zhang et al. 2018; Jung et al. 2019; Zhou et al. 2016; Jacob et al. 2018a; Han, Mao, and Dally 2016), their widespread adoption has been hindered due to dependencies on re-training, the necessity of a complete dataset, and sophisticated hyper-parameter tuning.

Post-training quantization methods, which convert high-precision representation bits to low-precision bits without requiring re-training steps, have been extensively studied by researchers and widely adopted in practical scenarios (Jiang et al. 2021; Choukroun et al. 2019; Nagel et al. 2019; Zhao et al. 2019; Lee et al. 2018; Goncharenko et al. 2019; Meller et al. 2019; Migacz 2017; Wu et al. 2020b). PTQ helps in the rapid deployment of CNN models on resource-constrained devices by addressing time-consuming and data privacy issues. However, PTQ leads to significant accuracy degradation, particularly in low-precision representations, and prior research has mainly focused on `int8` quantization. As an effort to preserve the performance of a full-precision model, recent PTQ works (Nagel et al. 2020; Li et al. 2021; Hubara et al. 2021; Wei et al. 2022; Wang et al.) have suggested to reconstruction error minimization of each layer or block by adjusting the magnitude of weight rounding and searching optimal scaling factors.

Recently, quantization for vision transformers has been studied (Liu et al. 2021b; Lin et al. 2022; Yuan et al. 2022; Ding et al. 2022; Liu et al. 2023). To reduce quantization error, such research works have considered the special structure of vision transformers such as multi-head attention and layer normalization. However, these approaches do not account for the distinctive characteristics of hybrid vision transformers, including the presence of bridge blocks and the utilization of diverse normalization techniques.

## Preliminary

### Hybrid Vision Transformers and Bridge Blocks

To address the inefficiencies of pure vision transformer models, MobileViTv1 was proposed as a hybrid, combining convolution and transformers to reduce model size without compromising accuracy.

**Variants of Hybrid Vision Transformers.** Following MobileViTv1’s release, several hybrid vision transformers emerged. MobileViTv2 refines the  $O(N^2)$  complexity attention map of MobileViTv1 to linear complexity. Mobile-Former integrates MobileNet and Transformer outputs. Efficient-FormerV1 employs a MetaBlock to eliminate latency-inefficient operators, while Efficient-FormerV2 reduces model parameters from V1 and introduces a design for better accuracy.

**Bridge Blocks.** The Bridge Block varies in its exact location depending on each hybrid vision model, but fundamentally consists of operators that adjust dimensions to facilitate transitions between local and global representations. Specifically, for MobileViTv1 and MobileViTv2, it implies convolution and reshape operators to align the input dimensions of the Transformer. In the case of Mobile-Former, it refers to operators within the Mobile-Former Block that transition bi-directionally between local and global representations. For Efficient-FormerV1, these are operators that convert meta-blocks from 4D to 3D. In the case of Efficient-FormerV2, the bridge block consists of local and global transition operators present in the 3rd and 4th stages.

### Hybrid Vision Transformer Quantization

Uniform quantization is a commonly used method to quantize neural networks, including convolution networks and transformers. As shown in Figure 1, quantization for hybrid vision transformers is divided into three parts: convolution, bridge block, and transformer. In uniform quantization, the weights and input activations are evenly quantized by each scale factor as:

$$\mathbf{x}_q = \mathcal{Q}(\mathbf{x}_r) = \text{clip}(\text{round}\left(\frac{\mathbf{x}_r}{\Delta_x} + zp\right), \text{min}, \text{max}), \quad (1)$$

where  $\mathbf{x}_r$  is a real value (full precision) and  $\mathbf{x}_q$  is a quantized value.  $\Delta_x$  is a scaling factor that is calculated depending on the quantization scheme: either asymmetric or symmetric. Also,  $zp$  denotes the zero point and exists only when using the asymmetric scheme.

In the case of transformers, input data is first passed through a quantized embedding layer before entering the transformer blocks, which consist of a multi-head self-attention (MHSA) and a feed-forward network (FFN). The MHSA module computes queries  $\mathbf{Q}$ , keys  $\mathbf{K}$ , and values  $\mathbf{V}$  with their pre-trained weights  $\mathbf{W}$  and inputs  $\mathbf{X}$ .

In a specific quantized transformer layer, the weights of  $\mathbf{Q}$ ,  $\mathbf{K}$ ,  $\mathbf{V}$  are quantized, and then multi-head self-attention is calculated using  $\mathbf{Q}$ ,  $\mathbf{K}$ , and softmax normalization. After the self-attention layer, FFN takes a quantized output which is concatenated from the results of MHSA as an input.

A popular method to reduce quantization error in post-training is reconstruction error minimization (Yuan et al. 2022; Nagel et al. 2020; Li et al. 2021; Ding et al. 2022). Previous works optimized task loss  $\mathcal{L} = \text{Cross Entropy}(\hat{\mathbf{y}}, \mathbf{y})$ , where  $\hat{\mathbf{y}}$  represents the quantized output and  $\mathbf{y}$  denotes the full precision output which is used as ground truth in PTQ. The expectation of task loss is a function of network parameters  $\mathbf{w}$ , given by  $\mathbb{E}[\mathcal{L}(\mathbf{x}, \mathbf{y}, \mathbf{w})]$ , where  $\mathbf{x}$  denotes activation and  $\mathbf{y}$  denotes output. Quantization introduces a small perturbation  $\epsilon$  on the parameter  $\hat{\mathbf{w}} = \mathbf{w} + \epsilon$ . As in prior works (Yuan et al. 2022; Nagel et al. 2020; Li et al. 2021; Ding et al. 2022), we calculate the influence of quantization on the task loss using Taylor series expansion as:

$$\mathbb{E}[\mathcal{L}(\mathbf{x}, \mathbf{y}, \hat{\mathbf{w}})] - \mathbb{E}[\mathcal{L}(\mathbf{x}, \mathbf{y}, \mathbf{w})] \approx \epsilon^\top \bar{g}^{(\mathbf{w})} + \frac{1}{2} \epsilon^\top \bar{H}^{(\mathbf{w})} \epsilon. \quad (2)$$

Since the weight perturbation  $\epsilon$  is relatively small, a second-order term of Taylor expansion can be used. In this

equation,  $\bar{g}^{(w)} = \mathbb{E}[\nabla_w \mathcal{L}(\mathbf{x}, \mathbf{y}, \hat{\mathbf{w}})]$  is the gradient and can be ignored if the pre-trained model is well-converged.  $\bar{H}^{(w)} = \mathbb{E}[\nabla_w^2 \mathcal{L}(\mathbf{x}, \mathbf{y}, \hat{\mathbf{w}})]$  is the Hessian matrix. The goal is to find a quantizer that includes optimal scaling factors or a rounding scheme to minimize the influence, given by  $\min \mathbb{E}[\mathcal{L}(\mathbf{x}, \mathbf{y}, \hat{\mathbf{w}})] - \mathbb{E}[\mathcal{L}(\mathbf{x}, \mathbf{y}, \mathbf{w})]$ . However, directly minimizing task loss leads to overfitting problems due to small datasets during the calibration phase. Thus, the second-order term of the Taylor series (Eq.(2)) is used. Referring to BRECQ (Li et al. 2021), to reduce computational cost, Eq.((2)) is simplified by removing the gradient ( $\bar{g}^{(w)}$ ) and approximating  $\epsilon = \Delta w$  to the network output ( $\Delta O = \hat{O} - O$ ) as:

$$\epsilon^\top \bar{H}^{(x)} \epsilon \approx \Delta O^\top \bar{H}^{(O)} \Delta O. \quad (3)$$

Referring to previous works (Yuan et al. 2022; Nagel et al. 2020; Li et al. 2021; Ding et al. 2022), MSE minimization based on the squared gradient that approximates the Hessian matrix captures the trend of task loss more accurately than other metrics such as MSE, Cosine, and Pearson.

We adopt the methodology described in (Yuan et al. 2022; Ding et al. 2022; Wu et al. 2020a) to traverse a search space of scaling factors by linearly dividing the maximum-minimum range of  $w$  and  $x$  into  $n$  candidates as:

$$\begin{aligned} & \left[ \alpha \frac{\text{MAX}|\mathbf{w}_l|}{2^{k-1}}, \beta \frac{\text{MAX}|\mathbf{w}_l|}{2^{k-1}} \right] \\ & \left[ \alpha \frac{\text{MAX}|\mathbf{x}_l|}{2^{k-1}}, \beta \frac{\text{MAX}|\mathbf{x}_l|}{2^{k-1}} \right], \end{aligned} \quad (4)$$

where  $\alpha$  and  $\beta$  are utilized to control the number of candidates generated for scaling factors.

## Challenges of Hybrid ViT Quantization

Here, we identify four critical challenges (C1–C4) that impede the quantization of hybrid vision transformers and explain why the current quantization method is insufficient.

### C1: Highly Dynamic Activation Range

To mitigate the decline in accuracy caused by highly dynamic activation ranges, the granularity of quantization should be changed adaptively according to the channel distribution of each layer. For layers that exhibit different ranges per channel, a per-channel scaling factor could be chosen to preserve a specific layer (Wu et al. 2020b). Otherwise, channels exhibiting a narrow range might encounter the problem where all values are treated as zeros during the application of layer-wise quantization.

To this end, channel-wise granularity is good for highly dynamic activations across channels. When prioritizing accuracy preservation without considering latency, opting for a fine-grained granularity at the channel level could yield the highest accuracy. However, *this does not always hold true in the hybrid vision transformers*. Applying channel-wise quantization to all the layers rather causes the scaling factors to overfit to small calibration data. This exacerbates the disparity between validation and calibration, resulting in a severe accuracy drop. Figure 2 shows the phenomenon where scaling factors, determined on a channel-wise basis during

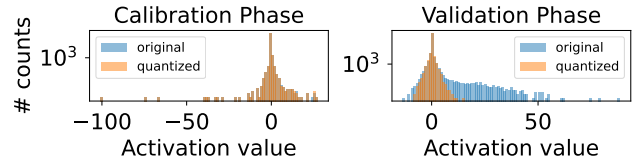


Figure 2: Discrepancy in activation ranges between the calibration and validation datasets in 1st bridge block of MobileViTv2-100

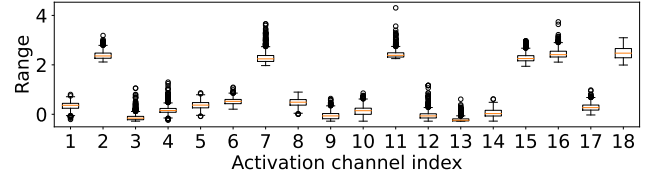


Figure 3: Per activation channel ranges of convolution in bridge block of MobileViTv1-xxs

the calibration phase, exhibit discrepancies during the validation phase. As a result, simply applying channel-wise granularity for quantization across all layers is problematic in hybrid ViTs. For layers where overfitting is an issue, applying the scaling factor on a layer-wise basis can alleviate this problem. Therefore, determining the optimal granularity of the scaling factor is a critical consideration.

### C2: Zero-point Overflow in Bridge Block

Uniform quantization includes two types: asymmetric and symmetric quantization, each with its own advantages and disadvantages. In most cases, asymmetric quantization shows better accuracy than symmetric quantization. But, we found that *a severe accuracy drop occurs in the bridge block when using an asymmetric scheme or channel-wise granularity* due to highly dynamic activation ranges according to each channel and non-zero distribution. This observation aligns with the prior discovery that adopting fine-grained granularity, such as channel-wise, does not always lead to minimal quantization error.

As shown in Figure 3, the activation of the bridge block convolution shows a similar range for both the maximum and minimum values across all channels, indicating that layer-wise quantization does not lead to significant accuracy degradation. However, when applying channel-wise quantization to distributions such as the 2nd, 7th, 11th, and so on in Figure 3, where all values are greater than zero, overflow of zero-point value for asymmetric quantization occurs (i.e., the zero-point value exceeded between  $-128$  and  $127$ ). As shown in Figure 4, the clipped zero point is used, resulting in certain values being reconstructed as a single value. These issues manifest differently across models, necessitating an automated approach to choosing granularity and scheme.

### C3: Quantization with Diverse Normalizations

*Hybrid vision transformers, unlike pure models such as CNN and ViT, employ different combinations of normalization techniques.* In the case of MobileViTv1, Mobile-Former, EfficientFormerV1, and EfficientFormerV2, BatchNorm and

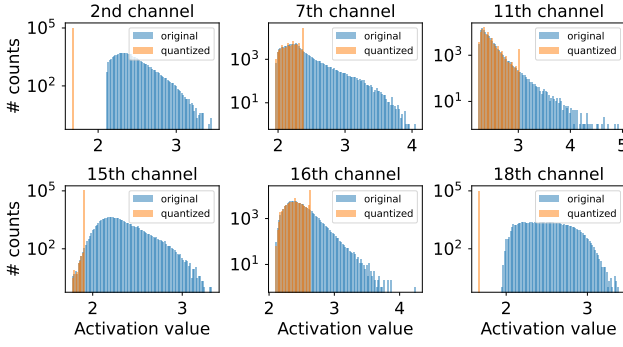


Figure 4: The selected problematic activation channels of convolution in bridge block of MobileViTv1-xxs due to overflow of zero point when using the channel-wise manner and asymmetric scheme

LayerNorm are utilized, while MobileViTv2 uses BatchNorm and GroupNorm. In order to create a network that is as parameter-efficient as possible, various normalizations are used in each hybrid vision transformer. However, a method to quantize all the normalizations used has not yet been proposed. Unlike BatchNorm, the computation of LayerNorm, GroupNorm, and InstanceNorm requires dynamic computation to determine the mean and variance. When dynamic operations are handled in a floating point, additional data movement occurs in off-chip memory. Therefore, to minimize the inference latency, the normalization should be quantized so that as many dynamic operations as possible can be processed in the integer domain.

#### C4: Sub-5M Parameter Models

Compared to heavy CNN models such as ResNet and VGG series, lightweight models with a relatively small number of parameters and few residual connections are more susceptible to the quantization process. *This vulnerability is particularly pronounced in models that have fewer than 5M parameters, where the quantization error is significantly higher in hybrid vision transformers.* As previously mentioned, using an asymmetric scheme for an activation distribution with a minimum value of 0 or greater can cause force clamping due to the zero point overflow problem, making the accuracy very sensitive to the quantization granularity and scheme.

### Methodology

Addressing the four identified challenges (C1–C4), we design Q-HyViT, a precise post-training quantization framework specifically tailored for hybrid ViTs. It automatically identifies optimal layer-wise strategies – choosing granularity (channel-wise or layer-wise) for C1 and C2, quantization scheme (symmetric or asymmetric) for C2, and quantization scaling factor for C3 and C4. This is achieved by leveraging the proposed hybrid reconstruction error minimization technique in the following section, also illustrated in Figure 1.

#### Hybrid Reconstruction Error Minimization

Previous post-training quantization methods for ViTs have typically aimed to optimize the quantization task loss, which

is achieved through the utilization of reconstruction error minimization, relying on second-order metrics to assess potential scaling factors for quantization. Furthermore, these methods incorporate a weight-rounding mechanism to enhance the overall quantization process. However, faced with the challenges specific to hybrid vision transformers, they become less effective in dealing with *bridge blocks*, which contain a gap between local and global representation, and *high dynamic activation ranges* resulting from the mixed structure of CNN and transformer.

To address these issues, Q-HyViT introduces *hybrid reconstruction error minimization*, which distinguishes the reconstruction strategy based on whether a given layer is part of the bridge block or not. It then determines the appropriate granularity and quantization scheme for each layer during post-training quantization. The reconstruction objective ( $O^{bb}$ ) of the hybrid approach can be represented as:

$$O^{bb} = \begin{cases} \mathbf{w}_n^{bb} \mathbf{w}_{n-1}^{bb} \dots \mathbf{w}_1^{bb} \mathbf{x}^{bb}, & \text{if a layer is in a bridge block} \\ \mathbf{w}^\ell \mathbf{x}^\ell, & \text{otherwise } bb \text{ is equal to } \ell \end{cases} \quad (5)$$

When a layer is part of the bridge block, the objective encompasses all the preceding layers within that bridge block.

Moreover, our hybrid reconstruction not only enables hybrid ViTs to achieve minimal quantization errors, but also determines quantization granularity and scheme automatically for each layer, using the hybrid reconstruction equation, guided by the reconstruction objective:

$$\begin{aligned} \min_{\Delta, g, s} \mathbb{E} \left[ \Delta O^{(bb), \tau}, \mathbf{H}^{O^{(bb)}} \Delta O^{(bb)} \right] \approx \\ \min_{\Delta, g, s} \mathbb{E} \left[ \Delta O^{(bb), \tau}, \text{diag} \left( \left( \frac{\partial L}{\partial O_1^{(bb)}} \right)^2, \dots, \left( \frac{\partial L}{\partial O_{|O^{bb}|}^{(bb)}} \right)^2 \right) \Delta O^{(bb)} \right], \end{aligned} \quad (6)$$

where  $bb$  is  $\in [BridgeBlock, a \text{ layer}]$ . In Eq. (6),  $\Delta O^{(bb)}$  is the difference between before and after quantization outputs.  $O_n^{(bb)}$  indicates the  $n$ -th element of  $O^{bb}$ . the range of  $n$  is from 1 to  $|O^{bb}|$ . As a result, we optimize the optimal scaling factor ( $\Delta \in [1, 100]$ ), granularity ( $g \in [layer, channel]$ ), and scheme ( $s \in [asymmetric, symmetric]$ ) through hybrid reconstruction error minimization.

#### Q-HyViT Framework

The proposed Q-HyViT method, as outlined in Algorithm 1, leverages hybrid reconstruction to determine optimal scaling factors, granularity, and scheme. Thus, it effectively diminishes quantization errors in hybrid ViTs. Throughout the calibration process, Q-HyViT calculates the output and gradient of each bridge block and layer through forward and backward propagation and then optimizes all hybrid transformer layers by reducing reconstruction error. As we mentioned, in the hybrid ViTs, the dynamic activation range varies widely, necessitating the need for automatic adjustment methods. From this perspective, this approach minimizes quantization errors to improve the second-order metric and ultimately leads to more accurate models.

---

**Algorithm 1:** The tuning process of Q-HyViT

---

**Input:** Hybrid vision transformer model and a few images for calibration;  
**Output:** Optimal scaling factors( $\Delta^*$ ) scheme( $s$ ) and granularity( $g$ );

```

1 while a layer( $\ell$ ) is not the end of layer do
2   /* full-precision outputs on each
   layer including final layer
   ( $\mathbf{y}^{(fp32)}$ ) */ 
3    $O_\ell^{bb} \leftarrow$  forward propagation ( $\mathbf{w}_\ell \mathbf{x}_\ell$ )
4 end
5 while a layer( $\ell$ ) is not the end of layer do
6   if a layer( $\ell$ ) in a Bridge Block then
7     Backward propagation to get  $\frac{\partial \mathcal{L}}{\partial O^{bb}}$ 
8   end
9   else
10    Backward propagation to get  $\frac{\partial \mathcal{L}}{\partial O^\ell}$ 
11 end
12 while a layer( $\ell$ ) is not the end of layer do
13   /* initialize scaling factors */ 
14    $\Delta_{\mathbf{w}_\ell^{bb}}^*, \Delta_{\mathbf{x}_\ell^{bb}}^* \leftarrow \frac{\text{MAX}(|\mathbf{w}_\ell^{bb}|)}{2^k}, \frac{\text{MAX}(|\mathbf{x}_\ell^{bb}|)}{2^k}$ 
15   /* Generate candidates for scaling
   factors */ 
16    $\Delta_{\mathbf{w}_\ell^{bb}}, \Delta_{\mathbf{x}_\ell^{bb}} \leftarrow$  Eq. (4)
17   while Three iterations do
18     /* Determine granularity,
     scheme, scaling factors */ 
19      $g, s, \Delta_{\mathbf{w}_\ell^{bb}}^*, \Delta_{\mathbf{x}_\ell^{bb}}^* \leftarrow$  Eq. (6)
20   end
21 end
22 return  $\Delta^*, g, s$ 

```

---

## Evaluation

We conduct an extensive comparison of Q-HyViT against various existing quantization methods. As previously discussed, there is no comprehensive method to quantize the hybrid vision transformers, so we directly implement the following open-sourced state-of-the-art quantization algorithms for pure vision transformers, namely EasyQuant (Wu et al. 2020a), FQ-ViT (Lin et al. 2022), and PTQ4ViT (Yuan et al. 2022), and then apply them on five hybrid vision transformer architectures.

## Accuracy Evaluation

We select MobileViTv1 (Mehta and Rastegari 2021), MobileViTv2 (Mehta and Rastegari 2022), Mobile-Former (Chen et al. 2022), EfficientFormerV1 (Li et al. 2022), and EfficientFormerV2 (Li et al. 2023) as representative hybrid vision transformer architectures.

**Results with Partial Quantization.** Table 1 shows quantization results on hybrid ViT architectures with varying model sizes, in terms of 8-bit and 6-bit quantization, where softmax and layer-norm remain under floating-point.

Upon examining the table, it is evident that previous

Table 1: A comparison of three post-training quantization methods for image classification on ImageNet-1K using five hybrid ViT architectures and bit-widths. In quantized models, softmax and layer-norm remain under floating-point. We abbreviate MobileViT as "MV", Mobile-Former as "MF", and EfficientFormer as "EF"

Model	# Params.	Type	FP32	EasyQuant		PTQ4ViT		Ours	
				W8A8	W6W6	W8A8	W6W6	W8A8	W6W6
MVv1-xxs	1.3M	Hybrid	69.0	36.13	10.17	37.75	30.80	68.20	66.33
MVv1-xs	2.3M	Hybrid	74.8	73.16	55.22	65.52	62.56	74.31	73.44
MVv1-s	5.6M	Hybrid	78.4	74.21	42.70	68.19	65.07	77.92	77.18
MVv2-050	1.4M	Hybrid	70.2	66.80	11.58	39.39	45.38	69.89	69.07
MVv2-075	2.8M	Hybrid	75.6	62.91	2.54	65.54	65.85	75.29	74.58
MVv2-100	4.9M	Hybrid	78.1	69.34	0.12	51.02	47.27	77.63	77.11
MVv2-125	7.5M	Hybrid	79.6	77.31	4.56	67.39	59.39	79.31	77.03
MVv2-150	10.6M	Hybrid	80.4	75.83	10.39	68.61	67.58	80.09	79.97
MVv2-175	14.3M	Hybrid	80.8	79.93	47.22	72.30	71.78	80.63	80.45
MVv2-200	18.5M	Hybrid	81.2	80.04	57.32	75.50	74.65	80.94	80.76
MF-26m	3.2M	Hybrid	64.0	28.95	0.12	58.27	47.25	61.78	47.25
MF-52m	3.5M	Hybrid	68.7	62.16	17.29	67.32	62.01	67.79	62.01
MF-96m	4.6M	Hybrid	72.8	53.31	33.68	71.32	64.72	71.60	64.72
MF-151m	7.6M	Hybrid	75.2	4.98	3.49	73.86	68.16	74.30	68.16
MF-214m	9.4M	Hybrid	76.7	72.79	28.32	75.01	68.24	75.76	68.24
MF-294m	11.4	Hybrid	77.9	74.15	59.55	76.96	68.24	76.93	74.48
MF-506m	14.0M	Hybrid	79.3	78.01	67.14	75.44	70.13	75.60	70.13
EFv1-L1	12.3M	MetaBlock	80.2	78.24	58.83	80.11	79.8	80.15	77.25
EFv1-L3	31.3M	MetaBlock	82.4	82.39	80.38	82.39	82.36	82.46	82.18
EFv1-L7	82.1M	MetaBlock	83.3	83.24	81.89	83.34	83.16	83.31	83.12
EFv2-S0	3.5M	Hybrid	76.2	68.21	41.24	68.40	41.26	74.69	74.18
EFv2-S1	6.1M	Hybrid	79.7	66.42	2.69	73.44	73.34	77.56	77.54
EFv2-S2	12.6M	Hybrid	82.0	71.80	7.02	79.85	79.39	80.62	80.30
EFv2-L	26.1M	Hybrid	83.5	80.34	3.34	82.46	82.22	82.80	82.71

Table 2: Fully quantized accuracy of hybrid vision transformer architectures.

Model	# Params.	Type	FP32	FQ-ViT	Ours
MobileViTv1-xxs (MVv1-xxs)	1.3M	Hybrid	68.91	0.1	67.20
MobileViTv1-xs (MVv1-xs)	2.3M	Hybrid	74.64	62.2	73.89
MobileViTv1-s (MVv1-s)	5.6M	Hybrid	78.31	74.94	77.72
MobileViTv2-050 (MVv2-050)	1.4M	Hybrid	70.16	5.00	68.73
MobileViTv2-075 (MVv2-075)	2.8M	Hybrid	75.62	34.60	74.36
MobileViTv2-100 (MVv2-100)	4.3M	Hybrid	78.09	0.40	77.13

works have experienced a significant decrease in accuracy, even with 8-bit quantization, in hybrid vision transformers. PTQ4ViT and EasyQuant perform fairly well by exploring scaling factors for each layer using Hessian and Cosine similarity to minimize reconstruction error when the model size is large. However, for models with fewer than 5M parameters, such as extremely lightweight models, existing quantization methods inadequately address dynamic activation changes. This leads to significant accuracy degradation, even in 8-bit settings. In contrast, our Q-HyViT achieves less than 1% accuracy drop with 8-bit quantization on the sub-5M models including xxs, xs, 050, 075, 100, 26m, 52m, 96m, and S0. In summary, Q-HyViT exhibits average improvements of 9.54% and 7.09% over EasyQuant and PTQ4ViT, respectively, with an 8-bit setting. Under the 6-bit setup, the improvements reach 43.39% and 8.65%, respectively.

Specifically, MobileViTv2 shows more accuracy drop than MobileViTv1 at the same model size, potentially due to its use of linear attention in self-attention computation, which results in fewer attention maps and lower resilience after post-softmax values. In the case of EfficientFormerV1, there is no significant difference between the conventional

Table 3: Ablation study on hybrid reconstruction error minimization, where  $\checkmark$  denotes that the component is considered. Results without employing all components are for FQ-ViT.

Model	Scale Factor	Granularity	Quant. Scheme	Accuracy
MobileViTv1-xxs	$\times$	$\times$	$\times$	37.75
	$\checkmark$	$\times$	$\times$	44.37
	$\checkmark$	$\checkmark$	$\times$	59.50
MobileViTv1-xs	$\checkmark$	$\checkmark$	$\checkmark$	68.20
	$\times$	$\times$	$\times$	65.52
	$\checkmark$	$\times$	$\times$	69.12
MobileViTv1-s	$\checkmark$	$\checkmark$	$\times$	72.00
	$\checkmark$	$\checkmark$	$\checkmark$	74.31
	$\times$	$\times$	$\times$	68.19
MobileViTv2-050	$\checkmark$	$\times$	$\times$	73.02
	$\checkmark$	$\checkmark$	$\times$	77.01
	$\checkmark$	$\checkmark$	$\checkmark$	77.92
MobileViTv2-075	$\times$	$\times$	$\times$	39.39
	$\checkmark$	$\times$	$\times$	49.62
	$\checkmark$	$\checkmark$	$\times$	69.89
MobileViTv2-100	$\checkmark$	$\times$	$\times$	65.54
	$\checkmark$	$\checkmark$	$\times$	67.24
	$\checkmark$	$\checkmark$	$\checkmark$	75.29
MobileViTv2-125	$\times$	$\times$	$\times$	51.02
	$\checkmark$	$\times$	$\times$	68.18
	$\checkmark$	$\checkmark$	$\times$	77.63
MobileViTv2-150	$\checkmark$	$\times$	$\times$	67.39
	$\checkmark$	$\checkmark$	$\times$	75.39
	$\checkmark$	$\checkmark$	$\checkmark$	79.31
MobileViTv2-175	$\times$	$\times$	$\times$	68.61
	$\checkmark$	$\times$	$\times$	75.88
	$\checkmark$	$\checkmark$	$\times$	80.09
MobileViTv2-200	$\checkmark$	$\times$	$\times$	72.30
	$\checkmark$	$\checkmark$	$\times$	76.81
	$\checkmark$	$\checkmark$	$\checkmark$	80.63

method and the proposed method. The reason for this is that in the meta block, convolution and transformer layers are not used in a hybrid manner. Furthermore, we observe that larger hybrid vision transformers are less sensitive to low-bit quantization (6-bit), as evidenced by the accuracy drops of MobileViTv1-xxs, MobileViTv1-xs, and MobileViTv1-s, which are 2.67, 1.36, and 1.22, respectively. This pattern is also observed in MobileViTv2, Mobile-Former, EfficientFormerV1, and EfficientFormerV2. This phenomenon is attributed to larger networks having more weights and generating more activations, making them more resilient to perturbations caused by quantization.

**Results with Full Quantization.** Previous studies (Liu et al. 2021b; Yuan et al. 2022; Wu et al. 2020a; Ding et al. 2022) have refrained from quantizing softmax and layer normalization operations due to their smaller computational demand compared to matrix multiplication in terms of total FLOPs. Moreover, straightforward quantization of such non-linear functions may result in considerable accuracy degradation. Nonetheless, integer-only quantization (Jacob et al. 2018b) is important especially for edge and mobile devices. This is due to the fact that softmax operation and layer

normalization require dequantization for their computation in floating-point, as well as data movement involved in off-chip memory. Thus, a fully quantized approach is necessary to alleviate significant hardware design challenges that arise from reducing off-chip level data transfer.

In line with previous research (Lin et al. 2022), we apply a fully quantized approach, FQ-ViT, to hybrid ViTs, as summarized in Table 2. Note that FQ-ViT shows very poor accuracy due to its use of an asymmetric scheme with zero points, which fails to handle the high variation of activation range by adjusting quantization granularity. Furthermore, in the case of MobileViTv2, group normalization is utilized instead of batch and layer norms, causing the existing L2 norm-based scaling factor exploration to function inaccurately. Our study addresses these issues and achieves an average of 43.63% accuracy improvement over FQ-ViT.

### Ablation Study on Hybrid Reconstruction

We perform an ablation study to assess the impact of utilizing the optimal selection of scale factor, granularity, and quantization scheme within the context of hybrid reconstruction error minimization. Table 3 provides a summary of the ablation study results for various sizes and types of hybrid vision transformer architectures, where the results demonstrate that all the components enhance the accuracy of quantized hybrid ViTs.

When only optimizing the scaling factor with hybrid reconstruction error minimization, it does not yield significant performance improvements compared to PTQ4ViT (baseline). However, optimizing not only the scaling factors but also the granularity and scheme based on the bridge block lead to synergistic effects in general. As a result, combining them all together leads to significant accuracy improvements. In contrast, excluding the optimization of granularity significantly decreases the accuracy, highlighting highly dynamic activation ranges in lightweight hybrid ViTs as the main cause of the accuracy drop.

### Conclusion

We addressed the problem of democratizing vision transformers on resource-constrained devices by proposing a method for minimizing quantization errors in hybrid vision transformers. The proposed method, Q-HyViT, identified the challenges of applying post-training quantization (PTQ) to hybrid vision transformers and proposed a unified method to mitigate errors in PTQ. Q-HyViT achieved this by selecting optimal scale factors, granularity, and scheme for both bridge and non-bridge layers based on hybrid reconstruction error minimization from a loss degradation perspective. We demonstrated the effectiveness of Q-HyViT by conducting extensive experiments comparing it with existing several open-source algorithms, EasyQuant, FQ-ViT, and PTQ4ViT, on the same hybrid vision transformers. The results showed that Q-HyViT outperformed existing methods by a significant margin and achieved state-of-the-art accuracy on hybrid vision transformers in a fully quantized manner, including non-linear operations such as softmax and diverse normalization. Finally, we contributed to the field of artificial intel-

lience by identifying the four unique challenges of quantizing hybrid vision transformers and proposing an effective solution for minimizing quantization error.

## Appendix

### Implementation Details

For a fair comparison, we maintain most configurations consistent with EasyQuant, PTQ4ViT, and FQ-ViT. Specifically, our settings vary depending on whether the model is fully quantized or not. Additionally, the 5 hybrid vision transformer models are referred to as the official models.

### Model Download

Except for Mobile-Former, the other four hybrid models leverage the `timm` framework<sup>2</sup>. Meanwhile, Mobile-Former is built upon the implementation by AAboys<sup>3</sup>. We successfully replicated the original accuracy using open-source codes under FP32 precision.

### Settings for EasyQuant and PTQ4ViT

In EasyQuant, we quantize all operators, including fully-connected layers and matrix multiplications. To obtain the optimal scaling factors, we employ a search algorithm based on cosine distance. The search space is derived from  $\alpha = 0.5$  and  $\beta = 1.2$ .

In PTQ4ViT, we adjust the hyperparameters to  $\alpha = 0$  and  $\beta = 1.2$ . Similar to PTQ4ViT, this study adopts the parallel quantization method to prevent a significant accuracy drop caused by small datasets.

### Settings for FQ-ViT

Essentially, we perform symmetric quantization on a per-channel basis for weights and asymmetric quantization on a per-layer basis for activations. To ensure a fair comparison, we set the quantization for weights to the minimum and maximum values. The hyperparameter K in the Power-of-Two Factor remains unchanged. For the calibration process, we select a sample of 1,000 images.

### Settings for Q-HyViT

We quantize all the weights and inputs for the fully connected layers, including the first projection layer and the last head layer. Additionally, the two input matrices for the matrix multiplications in the self-attention modules are quantized. The inputs of the softmax and normalization layers are also quantized, consistent with FQ-ViT. We use 32 images for calibration, and unoptimized scaling factors are initialized with minimum and maximum values.

### Bridge Block Details

The term `bridge block` refers to the transitional part that connects both convolution and transformer blocks. This block's precise configuration changes significantly among hybrid ViT structures. Table 4 lists detailed descriptions and

<sup>2</sup><https://github.com/huggingface/pytorch-image-models>

<sup>3</sup><https://github.com/AAboys/MobileFormer>

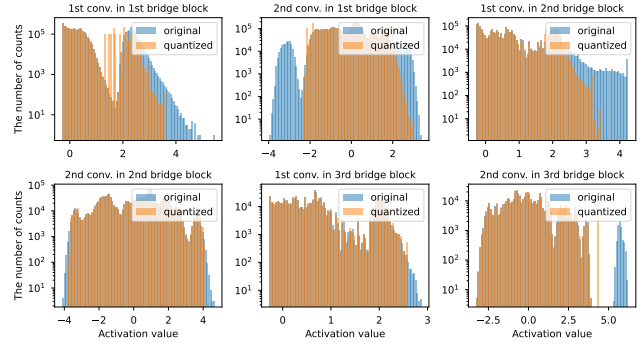


Figure 5: A histogram depicting the overlap between quantized values (blue) and real values (orange) for six activation layers in the 1st, 2nd, and 3rd bridge blocks of the MobileViTv1-xxs model

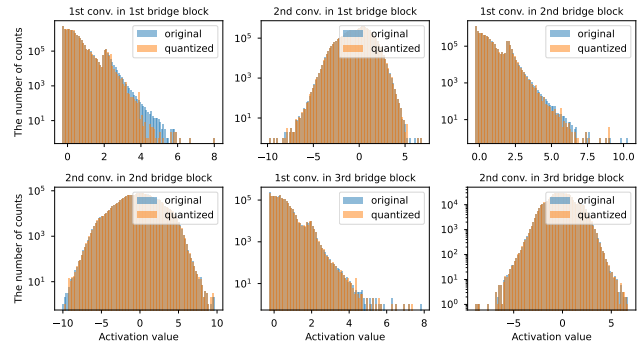


Figure 6: A histogram depicting the overlap between quantized values (blue) and real values (orange) for six activation layers in the 1st, 2nd, and 3rd bridge blocks of the MobileViTv1-xs model

operator names for each model. For MobileFormer, EfficientFormerV1, and EfficientFormerV2, the exact names of the operators that compose the bridge block vary slightly depending on the size of the model. The names shown in Table 4 are based on the smallest model size.

### Accuracy Variation in the calibration dataset

As listed in Tables 1 (partial quantization) and 2 (full quantization), the accuracy of each model varies depending on whether the softmax and layer-norm are quantized and the number of images utilized during the calibration phase. For a fair comparison with EasyQuant and PTQ4ViT as shown in Table 1, 32 images were employed to derive the results. In the case of FQ-ViT, the calibration utilized the 1,000 images referenced in the original paper. When increasing the number of images for calibration in partial quantization from 32 to 128, there is no significant difference in accuracy, as listed in Table 5.

Table 4: Definition and precise configuration of the Bridge Block within each hybrid vision transformer

Model	Description	Detailed Operators	# of Bridge Blocks
MobileViTv1	Convolution and reshape operators to align the input dimensions of the Transformer	stages.2.1.convkxk.conv -> stages.2.1.convix1 stages.3.1.convkxk.conv -> stages.3.1.convix1 stages.4.1.convkxk.conv -> stages.4.1.convix1	3
MobileViTv2	Convolution and reshape operators to align the input dimensions of the Transformer	stages.2.1.convkxk.conv -> stages.2.1.convix1 stages.3.1.convkxk.conv -> stages.3.1.convix1 stages.4.1.convkxk.conv -> stages.4.1.convix1	3
Mobile-Former	It refers to operators within the Mobile-Former Block that transition bi-directionally between local and global representations	features.1.local_global.proj -> features.1.global_block.ffn.0 features.1.global_local.proj -> features.2.conv1.0 features.2.local_global.proj -> features.2.global_block.ffn.0 features.2.global_local.proj -> features.3.conv1.0 features.3.local_global.proj -> features.3.global_block.ffn.0 features.3.global_local.proj -> features.4.conv1.0 features.4.local_global.proj -> features.4.global_block.ffn.0 features.4.global_local.proj -> features.5.conv1.0 features.5.local_global.proj -> features.5.global_block.ffn.0 features.5.global_local.proj -> features.6.conv1.0 features.6.local_global.proj -> features.6.global_block.ffn.0 features.6.global_local.proj -> features.7.conv1.0 features.7.local_global.proj -> features.7.global_block.ffn.0 features.7.global_local.proj -> features.8.conv1.0 features.8.local_global.proj -> features.8.global_block.ffn.0	15
EfficientFormerV1	These are operators that convert feature maps from 4D Meta Block to 3D Meta Block	stages.2.blocks.5.mlp.fc2 -> stages.3.downsample.conv -> stages.3.blocks.0.mlp.fc1	1
EfficientFormerV2	The bridge block consists of local and global transition operators exist in the 3rd and 4th stages	stages.2.downsample.conv.conv -> stages.2.blocks.0.mlp.fc1.conv stages.3.downsample.attn.proj.conv -> stages.3.blocks.0.mlp.fc1.conv	2

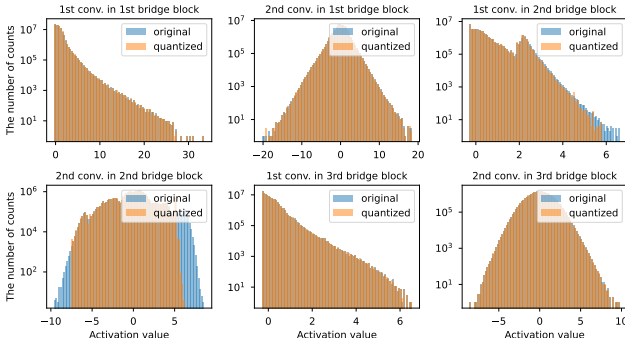


Figure 7: A histogram depicting the overlap between quantized values (blue) and real values (orange) for six activation layers in the 1st, 2nd, and 3rd bridge blocks of the MobileViTv1-s model

## Overflow Issues in Asymmetric Channel-wise Quantization

In this section, we demonstrate that the zero-point overflow issue arises across multiple bridge blocks within each hybrid vision transformer model. Two problematic activations are present in every bridge block. Both MobileViTv1 and MobileViTv2 comprise three bridge blocks. The distribution of activations before and after quantization for the convolution operations in each bridge block is illustrated in Fig.5, Fig.6, and Fig. 7.

From the three figures, we have discovered that the impact of zero point overflow diminishes as our models increase in size. This is due to the fact that the influence of zero point overflow decreases as the number of channels expands, such

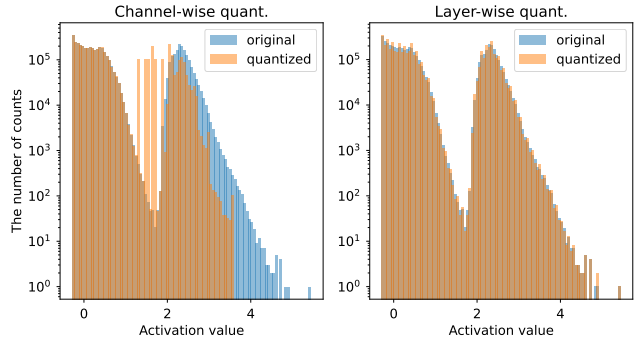


Figure 8: An overlapping histogram of quantized values (blue) and real values (orange) in the activation of for 1st bridge block of MobileViTv1-xxs: (left) channel-wise quantization (right) layer-wise quantization

as in the cases of 64 (xxs), 96 (xs), and 144 (s). Regardless of the model size, it is clear that clamping of specific values continues to occur in the bridge block. However, the accuracy drop issue is mitigated as the model size increases. In detail, for the FQ-ViT model, the accuracy is 0.1 for the xxs model, but it achieves accuracies of 62.2 and 74.94 for the xs and s models, respectively. In other words, although the same issue arises, as the model size increases, the impact on accuracy diminishes. The reason for this mitigation is that the number of redundant parameters increases as the size of the model increases. This is similar to why pruning works well for large models with many redundant parameters such as ResNet.

Additionally, for smaller models, we have observed that

Table 5: Quantization results under different numbers of calibration images. Partial means that softmax and layer-norm remain in floating-point, while full means that their operators are quantized

Model	Quant.	# of images	Accuracy
MobileViTv1-xxs	Partial	32	68.20
	Partial	128	68.18
	Full	500	67.16
	Full	1,000	67.20
MobileViTv1-xs	Partial	32	74.31
	Partial	128	74.25
	Full	500	73.82
	Full	1,000	73.89
MobileViTv2-s	Partial	32	77.92
	Partial	128	77.67
	Full	500	77.69
	Full	1,000	77.72
MobileViTv2-050	Partial	32	69.89
	Partial	128	69.89
	Full	500	68.52
	Full	1,000	68.73
MobileViTv2-075	Partial	32	75.29
	Partial	128	75.32
	Full	500	74.26
	Full	1,000	74.36
MobileViTv2-100	Partial	32	77.63
	Partial	128	77.75
	Full	500	77.19
	Full	1,000	77.13

the clamping issue associated with zero point overflow can be alleviated by transitioning from channel-wise quantization to layer-wise quantization, as demonstrated in Fig. 8. In the end, the reason why the zero point overflows are clamped is due to the following:

$$\begin{aligned}
 -128 &> q_{min} - \frac{r_{min}}{s} \\
 0 &> -\frac{r_{min}}{s} \\
 0 &< \frac{r_{min}}{s}
 \end{aligned} \tag{7}$$

In the above equation,  $q_{min}$  represents the minimum value of 8-bit quantization, which is  $-128$ ,  $s$  is the scaling factor, and  $r_{min}$  refers to the minimum value of the original activation. As shown in Eq. 7, since  $s$  is always a positive value, if  $r_{min}$  is greater than 0, the zero point exceeds the range of  $q_{min}$  and becomes clamped. Therefore, when quantizing on a per-channel basis, if activations are composed only of values greater than or equal to 0, it significantly causes a decrease in accuracy. To solve this issue, using layer-wise quantization takes into account the entire layer, including values less than or equal to 0 as  $r_{min}$ . Consequently, the zero-point value falls within the 8-bit range ( $-128$  to  $127$ ).

## References

- Banner, R.; Nahshan, Y.; and Soudry, D. 2019. Post training 4-bit quantization of convolutional networks for rapid-deployment. In Wallach, H.; Larochelle, H.; Beygelzimer, A.; d’Alché-Buc, F.; Fox, E.; and Garnett, R., eds., *Advances in Neural Information Processing Systems*, volume 32. Curran Associates, Inc.
- Chen, Y.; Dai, X.; Chen, D.; Liu, M.; Dong, X.; Yuan, L.; and Liu, Z. 2022. Mobile-former: Bridging mobilenet and transformer. In *Proceedings of the IEEE/CVF Conference on Computer Vision and Pattern Recognition*, 5270–5279.
- Choi, J.; Wang, Z.; Venkataramani, S.; Chuang, P. I.-J.; Srinivasan, V.; and Gopalakrishnan, K. 2018. Pact: Parameterized clipping activation for quantized neural networks. In *6th International Conference on Learning Representations, ICLR 2018, Vancouver, BC, Canada, April 30 - May 3, 2018, Conference Track Proceedings*. OpenReview.net.
- Chollet, F. 2017. Xception: Deep learning with depthwise separable convolutions. In *Proceedings of the IEEE conference on computer vision and pattern recognition*, 1251–1258.
- Choukroun, Y.; Kravchik, E.; Yang, F.; and Kisilev, P. 2019. Low-bit Quantization of Neural Networks for Efficient Inference. In *ICCV Workshops*, 3009–3018.
- Ding, Y.; Qin, H.; Yan, Q.; Chai, Z.; Liu, J.; Wei, X.; and Liu, X. 2022. Towards Accurate Post-Training Quantization for Vision Transformer. In *Proceedings of the 30th ACM International Conference on Multimedia*, 5380–5388.
- Dosovitskiy, A.; Beyer, L.; Kolesnikov, A.; Weissenborn, D.; Zhai, X.; Unterthiner, T.; Dehghani, M.; Minderer, M.; Heigold, G.; Gelly, S.; et al. 2020. An image is worth 16x16 words: Transformers for image recognition at scale. *arXiv preprint arXiv:2010.11929*.
- Esser, S. K.; McKinstry, J. L.; Bablani, D.; Appuswamy, R.; and Modha, D. S. 2020. Learned Step Size quantization. In *8th International Conference on Learning Representations, ICLR 2020, Addis Ababa, Ethiopia, April 26-30, 2020*, 1–12. OpenReview.net.
- Goncharenko, A.; Denisov, A.; Alyamkin, S.; and Terentev, E. 2019. Fast adjustable threshold for uniform neural network quantization. *International Journal of Computer and Information Engineering*, 13(9): 495–499.
- Han, K.; Wang, Y.; Chen, H.; Chen, X.; Guo, J.; Liu, Z.; Tang, Y.; Xiao, A.; Xu, C.; Xu, Y.; et al. 2022. A survey on vision transformer. *IEEE transactions on pattern analysis and machine intelligence*, 45(1): 87–110.
- Han, S.; Mao, H.; and Dally, W. J. 2016. Deep Compression: Compressing Deep Neural Network with Pruning, Trained Quantization and Huffman Coding. In Bengio, Y.; and LeCun, Y., eds., *4th International Conference on Learning Representations, ICLR 2016, San Juan, Puerto Rico, May 2-4, 2016, Conference Track Proceedings*.
- Howard, A.; Sandler, M.; Chu, G.; Chen, L.-C.; Chen, B.; Tan, M.; Wang, W.; Zhu, Y.; Pang, R.; Vasudevan, V.; et al. 2019. Searching for mobilenetv3. In *Proceedings of the IEEE/CVF international conference on computer vision*, 1314–1324.

- Howard, A. G.; Zhu, M.; Chen, B.; Kalenichenko, D.; Wang, W.; Weyand, T.; Andreetto, M.; and Adam, H. 2017. Mobilenets: Efficient convolutional neural networks for mobile vision applications. *arXiv preprint arXiv:1704.04861*.
- Hubara, I.; Nahshan, Y.; Hanani, Y.; Banner, R.; and Soudry, D. 2021. Accurate post training quantization with small calibration sets. In *International Conference on Machine Learning*, 4466–4475. PMLR.
- Jacob, B.; Kligys, S.; Chen, B.; Zhu, M.; Tang, M.; Howard, A.; Adam, H.; and Kalenichenko, D. 2018a. Quantization and training of neural networks for efficient integer-arithmetic-only inference. In *Proceedings of the IEEE Conference on Computer Vision and Pattern Recognition*, 2704–2713.
- Jacob, B.; Kligys, S.; Chen, B.; Zhu, M.; Tang, M.; Howard, A.; Adam, H.; and Kalenichenko, D. 2018b. Quantization and training of neural networks for efficient integer-arithmetic-only inference. In *Proceedings of the IEEE Conference on Computer Vision and Pattern Recognition*, 2704–2713.
- Jiang, Z.; Jain, A.; Liu, A.; Fromm, J.; Ma, C.; Chen, T.; and Ceze, L. 2021. Automated Backend-Aware Post-Training Quantization. *arXiv preprint arXiv:2103.14949*.
- Jung, S.; Son, C.; Lee, S.; Son, J.; Han, J.-J.; Kwak, Y.; Hwang, S. J.; and Choi, C. 2019. Learning to quantize deep networks by optimizing quantization intervals with task loss. In *Proceedings of the IEEE/CVF Conference on Computer Vision and Pattern Recognition*, 4350–4359.
- Khan, S.; Naseer, M.; Hayat, M.; Zamir, S. W.; Khan, F. S.; and Shah, M. 2022. Transformers in vision: A survey. *ACM computing surveys (CSUR)*, 54(10s): 1–41.
- Krishnamoorthi, R. 2018. Quantizing deep convolutional networks for efficient inference: A whitepaper. *arXiv preprint arXiv:1806.08342*.
- Lee, J. H.; Ha, S.; Choi, S.; Lee, W.-J.; and Lee, S. 2018. Quantization for rapid deployment of deep neural networks. *arXiv preprint arXiv:1810.05488*.
- Li, Y.; Gong, R.; Tan, X.; Yang, Y.; Hu, P.; Zhang, Q.; Yu, F.; Wang, W.; and Gu, S. 2021. Brecq: Pushing the limit of post-training quantization by block reconstruction. *arXiv preprint arXiv:2102.05426*.
- Li, Y.; Hu, J.; Wen, Y.; Evangelidis, G.; Salahi, K.; Wang, Y.; Tulyakov, S.; and Ren, J. 2023. Rethinking Vision Transformers for MobileNet Size and Speed. In *Proceedings of the IEEE international conference on computer vision*.
- Li, Y.; Yuan, G.; Wen, Y.; Hu, J.; Evangelidis, G.; Tulyakov, S.; Wang, Y.; and Ren, J. 2022. Efficientformer: Vision transformers at mobilenet speed. *Advances in Neural Information Processing Systems*, 35: 12934–12949.
- Lin, Y.; Zhang, T.; Sun, P.; Li, Z.; and Zhou, S. 2022. FQ-ViT: Post-Training Quantization for Fully Quantized Vision Transformer. In *Proceedings of the Thirty-First International Joint Conference on Artificial Intelligence, IJCAI-22*, 1173–1179.
- Liu, Y.; Yang, H.; Dong, Z.; Keutzer, K.; Du, L.; and Zhang, S. 2023. NoisyQuant: Noisy Bias-Enhanced Post-Training Activation Quantization for Vision Transformers. In *Proceedings of the IEEE/CVF Conference on Computer Vision and Pattern Recognition*, 20321–20330.
- Liu, Z.; Lin, Y.; Cao, Y.; Hu, H.; Wei, Y.; Zhang, Z.; Lin, S.; and Guo, B. 2021a. Swin transformer: Hierarchical vision transformer using shifted windows. In *Proceedings of the IEEE/CVF international conference on computer vision*, 10012–10022.
- Liu, Z.; Wang, Y.; Han, K.; Zhang, W.; Ma, S.; and Gao, W. 2021b. Post-training quantization for vision transformer. *Advances in Neural Information Processing Systems*, 34: 28092–28103.
- Ma, N.; Zhang, X.; Zheng, H.-T.; and Sun, J. 2018. Shufflenet v2: Practical guidelines for efficient cnn architecture design. In *Proceedings of the European conference on computer vision (ECCV)*, 116–131.
- Mehta, S.; and Rastegari, M. 2021. Mobilevit: light-weight, general-purpose, and mobile-friendly vision transformer. *arXiv preprint arXiv:2110.02178*.
- Mehta, S.; and Rastegari, M. 2022. Separable self-attention for mobile vision transformers. *arXiv preprint arXiv:2206.02680*.
- Meller, E.; Finkelstein, A.; Almog, U.; and Grobman, M. 2019. Same, Same But Different: Recovering Neural Network Quantization Error Through Weight Factorization. In Chaudhuri, K.; and Salakhutdinov, R., eds., *Proceedings of the 36th International Conference on Machine Learning*, volume 97 of *Proceedings of Machine Learning Research*, 4486–4495. PMLR.
- Migacz, S. 2017. 8-bit inference with tensorrt. In *GPU technology conference*, volume 2, 5.
- Nagel, M.; Amjad, R. A.; Van Baalen, M.; Louizos, C.; and Blankevoort, T. 2020. Up or down? adaptive rounding for post-training quantization. In *International Conference on Machine Learning*, 7197–7206. PMLR.
- Nagel, M.; Baalen, M. v.; Blankevoort, T.; and Welling, M. 2019. Data-free quantization through weight equalization and bias correction. In *Proceedings of the IEEE/CVF International Conference on Computer Vision*, 1325–1334.
- Sandler, M.; Howard, A.; Zhu, M.; Zhmoginov, A.; and Chen, L.-C. 2018. Mobilenetv2: Inverted residuals and linear bottlenecks. In *Proceedings of the IEEE conference on computer vision and pattern recognition*, 4510–4520.
- Tan, M.; Chen, B.; Pang, R.; Vasudevan, V.; Sandler, M.; Howard, A.; and Le, Q. V. 2019. Mnasnet: Platform-aware neural architecture search for mobile. In *Proceedings of the IEEE/CVF conference on computer vision and pattern recognition*, 2820–2828.
- Touvron, H.; Cord, M.; Douze, M.; Massa, F.; Sablayrolles, A.; and Jégou, H. 2021. Training data-efficient image transformers & distillation through attention. In *International conference on machine learning*, 10347–10357. PMLR.
- Wang, C.; Zheng, D.; Liu, Y.; and Li, L. ???? Leveraging Inter-Layer Dependency for Post-Training Quantization. In *Advances in Neural Information Processing Systems*.

- Wei, X.; Gong, R.; Li, Y.; Liu, X.; and Yu, F. 2022. QDrop: randomly dropping quantization for extremely low-bit post-training quantization. *arXiv preprint arXiv:2203.05740*.
- Wu, D.; Tang, Q.; Zhao, Y.; Zhang, M.; Fu, Y.; and Zhang, D. 2020a. EasyQuant: Post-training quantization via scale optimization. *arXiv preprint arXiv:2006.16669*.
- Wu, H.; Judd, P.; Zhang, X.; Isaev, M.; and Micikevicius, P. 2020b. Integer quantization for deep learning inference: Principles and empirical evaluation. *arXiv preprint arXiv:2004.09602*.
- Yuan, Z.; Xue, C.; Chen, Y.; Wu, Q.; and Sun, G. 2022. PTQ4ViT: Post-training Quantization for Vision Transformers with Twin Uniform Quantization. In *European Conference on Computer Vision*, 191–207. Springer.
- Zhang, D.; Yang, J.; Ye, D.; and Hua, G. 2018. Lq-nets: Learned quantization for highly accurate and compact deep neural networks. In *Proceedings of the European conference on computer vision (ECCV)*, 365–382.
- Zhao, R.; Hu, Y.; Dotzel, J.; De Sa, C.; and Zhang, Z. 2019. Improving neural network quantization without retraining using outlier channel splitting. In *International conference on machine learning*, 7543–7552. PMLR.
- Zhou, S.; Wu, Y.; Ni, Z.; Zhou, X.; Wen, H.; and Zou, Y. 2016. Dorefa-net: Training low bitwidth convolutional neural networks with low bitwidth gradients. *arXiv preprint arXiv:1606.06160*.